

Approved For Release STAT
2009/08/26 :
CIA-RDP88-00904R0001000110

Dec

Approved For Release
2009/08/26 :
CIA-RDP88-00904R0001000110



**Third United Nations
International Conference
on the Peaceful Uses
of Atomic Energy**

A/CONF.28/P/365

USSR

May 1964

Original: RUSSIAN

Confidential until official release during Conference

CALCULATION OF SLOW ENERGY NEUTRON SPECTRA

G.I. Marchuk, G.A. Iljasova, V.N. Morozov, V.V. Smelov, V.A. Hodakov.

There are three most essential aspects in the neutron thermalization problem: the development of the theory of neutron-matter interaction and the evaluation of corresponding constants, needed for calculation; the development of the computational algorithms for solving of mathematical problems with needed accuracy; and, at last, the problem of the interpretation of slow neutron flux spectral data. On the whole, in the present paper the questions of second aspect of the problem will be considered.

The slow energy neutron scattering problem was formulated by Hurwitz and Cohen [1,2]. The most complete solution of this problem was obtained in the theory of neutron scattering by nuclei of monoatomic gases [1-4]. In the last years the necessity turned out of a more careful analysis of neutron scattering mechanism, taking into account the molecular binding effect. The results of these investigations were reported in detail at the Brookhaven Conference on Neutron Thermalization [5].

It should be noted then that in the last years some important experimental data on the neutron thermalization problem have been obtained [5-7]. After these investigations the more careful comparison of experimental data with the theory based on different physical models is possible. It should be also observed that progress of our knowledge of physical processes in nuclear reactors makes the development of more perfect and exact methods of the solution of neutron transport equation evident.

The peculiarity of the problem of calculating the thermal neutron distribution lies in the fact, that the low energy neutrons not only lose their energy, but acquire it. Due to this effect, the integral operator in the transport equations is Fredholm-type operator. The transport equation may be solved by spherical harmonics method in P_n -approximation, by S_n -method, by the method of characteristics, by Monte Carlo method, and others [8-15].

The survey of some mathematical methods of solution of the transport equation, their confrontation and comparison of the theory with the experiment [6-7] are given in present paper. A special attention is paid to the problem of calculating neutron flux angular distributions in reactor cell.

25 YEAR RE-REVIEW

I. CALCULATION OF NEUTRON FLUX AND NEUTRON IMPORTANCE BY THE SPHERICAL HARMONICS METHOD.

The stationary slow neutron flux in the case of a cylindrical cell may be described by the following integro-differential transport equation:

$$\sin\theta(\cos\psi \frac{\partial\phi}{\partial r} - \frac{\sin\psi}{r} \frac{\partial\phi}{\partial\psi}) + a(r, v) \phi(r, v, \theta, \psi) - \int_0^{v_{\text{group}}} dv' \int d\Omega' a_s(r; v' \rightarrow v, \vec{\Omega}' \rightarrow \vec{\Omega}) \phi(r, v', \theta', \psi') = q(r, v) \quad (1)$$

where $a_s^0(r; v' \rightarrow v, \vec{\Omega}' \rightarrow \vec{\Omega})$ is the differential scattering cross-section; $a(r, v) = a_s(r, v) + a_a(r, v)$ is the total cross-section; θ and ψ are the meridional and azimuthal angles, respectively (Fig.1). Let the function $\phi(r, v, \theta, \psi)$ be in the form

$$\phi(r, v, \theta, \psi) = \rho(v) \nu(r, v, \theta, \psi) \quad (2)$$

where $\rho(v)$ is chosen to take a more complete account of the neutron flux $\phi(r, v, \theta, \psi)$ character of variation in variable v . The energy spectrum of formally homogenized cell was used as the function $\rho(v)$. From above one may conclude, that $\nu(r, v, \theta, \psi)$ is slightly dependent on the velocity v over the entire thermalization range $0 < v < v_{\text{group}}$.

Divide the range $0 < v < v_{\text{group}}$ into m intervals $v_j < v < v_{j+1}$ ($j=1, 2, \dots, m$). Within each energy group $v_j < v < v_{j+1}$ the function $\nu(r, v, \theta, \psi)$ can be approximately regarded as independent of neutron velocity. Then, substituting (2) in equation (1) and integrating the latter over everyone of the groups, we obtain the following system of equations:

$$\sin\theta(\cos\psi \frac{\partial\phi^{(j)}}{\partial r} - \frac{\sin\psi}{r} \frac{\partial\phi^{(j)}}{\partial\psi}) + a^{(j)}(r) \phi^{(j)}(r, \theta, \psi) - \sum_{l=1}^m \int \phi^{(l)}(r, \theta', \psi') a_s^{l \rightarrow j}(r, \vec{\Omega}' \rightarrow \vec{\Omega}) d\Omega' = q^{(j)}(r), \quad (1')$$

$$\text{where } \phi^{(j)}(r, \theta, \psi) = \int_{v_j}^{v_{j+1}} \phi(r, v, \theta, \psi) dv, \quad q^{(j)}(r) = \int_{v_j}^{v_{j+1}} q(r, v) dv,$$

$$a^{(j)}(r) = \frac{1}{\rho_j} \int_{v_j}^{v_{j+1}} a(v) \rho(v) dv, \quad \rho_j = \int_{v_j}^{v_{j+1}} \rho(v) dv$$

$$a_s^{l \rightarrow j}(r, \vec{\Omega}' \rightarrow \vec{\Omega}) = \frac{1}{\rho_j} \int_{v_e}^{v_{e+1}} \rho(v') dv' \int_{v_l}^{v_{l+1}} a_s(r, v' \rightarrow v, \vec{\Omega}' \rightarrow \vec{\Omega}) dv,$$

Let us expand the function $a_s^{l \rightarrow j}(r, \vec{\Omega}' \rightarrow \vec{\Omega})$ in Legendre polynomials

$$a_s^{l \rightarrow j}(r, \vec{\Omega}' \rightarrow \vec{\Omega}) = \frac{1}{2\pi} \sum_{n=0}^{\infty} \frac{2n+1}{2} a_n^{l \rightarrow j}(r) P_n(\mu_0) \quad (3)$$

$(\mu_0 = \cos(\vec{\Omega}', \vec{\Omega}))$, and neutron flux $\phi^{(i)}$ into spherical harmonics, so that

$$\begin{aligned} \phi^{(i)}(r, \theta, \psi) = & \frac{1}{2\pi} \sum_{n=0}^{\infty} \frac{2n+1}{2} \Phi_{n0}^{(i)}(r) P_n(\cos \theta) + \\ & + \frac{1}{2\pi} \sum_{n=1}^{\infty} \sum_{m=1}^n (2n+1) \frac{(n+m)!}{(n-m)!} \Phi_{nm}^{(i)}(r) \cos m\psi P_n^{(m)}(\cos \theta) \end{aligned} \quad (4)$$

P_3 is the approximation, when all $\Phi_{nm}^{(i)}(r)$ of $n > 4$ are neglected. Because of the scattering function $a_s^{l \rightarrow j}(r, \vec{\Omega}', -\vec{\Omega})$ independence of neither medium absorptivity nor of its size, in series (3) one may take into account only finite number of terms without connecting this fact with the order of approximation. For practice in (3) only two terms can be taken into account. As a result for each energy group we obtain the system of six differential equations for $\Phi_{nm}^{(i)}(r)$, which in a matrix form is x)

$$\left. \begin{aligned} a_0 \frac{dr_0}{dr} + \frac{1}{r} T_0 r + \Sigma \Phi &= S_0 \\ a_1 \frac{d\Phi}{dr} + \frac{1}{r} T_1 \Phi + \Sigma_1 r &= 3S_1 \end{aligned} \right\} \quad 3S_1 \quad (5)$$

where

$$\Phi = \begin{bmatrix} \Phi_{00} \\ \Phi_{20} \\ \Phi_{22} \end{bmatrix}, \quad r = \begin{bmatrix} \Phi_{11} \\ \Phi_{31} \\ \Phi_{33} \end{bmatrix}, \quad S_0 = \begin{bmatrix} S_{00} \\ 0 \\ 0 \end{bmatrix}, \quad S_1 = \begin{bmatrix} S_{11} \\ 0 \\ 0 \end{bmatrix}$$

$$S_{00}^{(i)}(r) = 4\pi q^{(i)}(r) + (1 - \delta_{je}) \sum_{l=1}^m \Phi_{00}^{(l)}(r) a_0^{l \rightarrow j}(r),$$

$$S_{11}^{(i)}(r) = (1 - \delta_{jl}) \sum_{l=1}^m \Phi_{11}^{(l)}(r) a_1^{l \rightarrow j}$$

$a_0, a_1, T_0, T_1, \Sigma_0, \Sigma_1$ are some matrix coefficients [10, 16].

Excluding the vector r from system (5), we obtain the equation:

$$\begin{aligned} D \frac{d^2 \Phi}{dr^2} + \frac{1}{r} K \frac{d\Phi}{dr} - (3\sigma_1 \Sigma_0 + \frac{1}{r^2} \wedge) \Phi &= \\ = -3\sigma_1 S_0 + 3V \left(\frac{dS_1}{dr} + \frac{1}{r} S_1 \right) - \frac{6}{r} W S_1 \end{aligned} \quad (6)$$

In equation (6): Σ_0, \wedge are diagonal matrixes,

$$\Sigma_0 = [\sigma_0, 5a, 5a/6] \quad \wedge = [0, 0, 4h]$$

^{x)} For the sake of simplicity, an index of the group number is omitted.

$$D = \begin{bmatrix} 1 & -1 & \frac{1}{2} \\ -1 & f & -\frac{g}{2} \\ 1 & -g & h \end{bmatrix}, \quad K = \begin{bmatrix} 1 & -1 & \frac{3}{2} \\ -1 & f & -\frac{3g}{2} \\ -1 & g & h \end{bmatrix},$$

$$V = \begin{bmatrix} 1 & 0 & 0 \\ -1 & 0 & 0 \\ 0 & 0 & 0 \end{bmatrix}, \quad W = \begin{bmatrix} 0 & 0 & 0 \\ 0 & 0 & 0 \\ 1 & 0 & 0 \end{bmatrix},$$

where $\sigma_0 = \alpha(i) - a_0^{i \rightarrow j}$, $\sigma_1 = \alpha(i) - a_1^{i \rightarrow j}$

$$f = 1 + \frac{18}{7} \frac{\sigma_1}{a}, \quad g = 1 + \frac{3}{7} \frac{\sigma_1}{a}, \quad h = \frac{1}{2} + \frac{4}{7} \frac{\sigma_1}{a}$$

Equations (6) are to be completed by the boundary conditions, providing symmetry of neutron flux at the cell centre and reflection condition at its boundary [10, 16].

The solution of system (6) is obtained by Zeidel iteration method. In this method the functions $S_{00}^{(j)}(r)$ and $S_{11}^{(j)}$ at n -th iteration step are calculated in the following scheme:

$$S_{00,n}^{(j)} = 4\pi q^{(j)}(r) + \sum_{e < j} \phi_{00,n-1}^{(l)} a_{01}^{l \rightarrow j} + \sum_{k > j} \phi_{00,n}^{(l)} a_{01}^{l \rightarrow j}$$

The solution of the multi-group theory must satisfy the neutron balance relation:

$$\sum_{j=1}^m \int_0^{R_{\text{group}}} a_d^{(j)}(r) \phi_{00}^{(j)}(r) r dr = \sum_{j=1}^m \int_0^{R_{\text{group}}} \phi_{00}^{(j)}(r) r dr \quad (7)$$

If the iterating is not accomplished, balance relation (7) is not achieved. If one trying to obtain balance relation (7) during the iteration process, it is possible to hasten considerably the convergence of the process [17]. In present paper it was made by the source renormalization.

Each onegroup equation of system (6) is solved by the method of the matrix factorization.

The functions $\phi_{00}^{(j)}(r) = \int \phi^{(j)}(r, \theta, \psi) d\Omega$, thus obtained, may be used for the calculation of effective thermal constants, needed for further calculations of critical reactor parameters. In some cases, however, it is important to know the angular dependence of the neutron flux $\phi^{(j)}(r, \theta, \psi)$. In some experimental investigations of thermal neutron spectra the neutron beams of the certain directions are used. Formula (4) reveals the possibility to calculate the neutron fluxes in any given direction. Below we cite the expressions of neutron fluxes with different velocity directions (see Fig.1).

$$\begin{aligned} \phi^{(j)}(r, \theta=0) &= \frac{1}{4\pi} [\phi_{00}^{(j)}(r) + 5\phi_{20}^{(j)}(r)], \\ \phi^{(j)}(r, \theta=\frac{\pi}{2}, \psi=\frac{\pi}{2}) &= \frac{1}{4\pi} [\phi_{00}^{(j)}(r) - \frac{5}{2}\phi_{20}^{(j)}(r) - \frac{5}{4}\phi_{22}^{(j)}(r)], \\ \phi^{(j)}(r, \theta=\frac{\pi}{2}, \psi=\frac{\pi}{4}) &= \frac{1}{4\pi} [\phi_{00}^{(j)}(r) - \frac{5}{2}\phi_{20}^{(j)}(r) + \frac{5}{4}\phi_{22}^{(j)}(r) \pm \\ &\pm (3\phi_{11}^{(j)}(r) - \frac{7}{4}\phi_{31}^{(j)}(r) + \frac{7}{24}\phi_{33}^{(j)}(r))]. \end{aligned} \quad (8)$$

After the neutron flux $\phi(r, v, \theta, \psi)$ the neutron importance $\phi^*(r, v, \theta, \psi)$ in relation to some process is of interest. For example, one can say about the neutron importance in relation to the

neutron absorption in block, etc.[18-20]. The neutron importance is a solution of the adjoint equation, which in multigroup representation has the form:

$$\sin\theta(\cos\psi \frac{\partial \phi^{*(j)}}{\partial r} - \frac{\sin\psi}{r} \frac{\partial \phi^{*(j)}}{\partial \psi}) + a^{(j)}(r)\phi^{*(j)}(r, \theta, \psi) - \sum_{l=1}^m \int \phi^{*(l)}(r, \theta', \psi') a_{s \rightarrow l}^{(j)}(r, \vec{\Omega} \rightarrow \vec{\Omega}') d\Omega' = q^{*(j)}(r, \theta, \psi) \quad (9)$$

The concrete form of the right side of equation (9) is connected with physical process in relation to which the neutron importance is determined. In particular, for the calculation of the neutron importance in relation to the block capture, one must put:

$$q^{*(j)}(r, \theta, \psi) = \begin{cases} a_a^{(j)}(r) & \text{in the block} \\ 0 & \text{beyond the block} \end{cases}$$

The solution of system (9) can be obtained by the same methods, as for system (1').

The neutron importance in the combination with the neutron flux distribution function is widely used in the perturbation theory [18,21].

II. CALCULATION OF NEUTRON FLUX BY S_n -METHOD.

To calculate the thermal neutron flux in a reactor cell, the S_n -method, proposed by Carlson [12,13], may be used successfully. In this section we shall discuss the application of this method to multigroup system (1'), the anisotropy of scattering will be taken into account only in transport approximation.

The solution of the corresponding system of equations with the reflection conditions at the cell boundary is realized by the following three types of iterating: inelastic transition iteration, elastic scattering iteration and boundary condition iteration. The equation iterated is of the form:

$$\sqrt{1-\gamma^2} \cos\psi \frac{\partial \phi_{s,t,r}^{(j)}}{\partial r} - \sqrt{1-\gamma^2} \frac{\sin\psi}{r} \frac{\partial \phi_{s,t,r}^{(j)}}{\partial \psi} + a_{tr}^{(j)}(r) \phi_{s,t,r}^{(j)} = Q_{s,t}^{(j)}(r) \quad (10)$$

where j is the energy group number ($j=1,2,\dots,m$), $\gamma=\cos\theta$,

$$Q_{s,t}^{(j)}(r) = \beta^{j \rightarrow j}(r) N_{s,t-1}^{(j)}(r) + Q_s^{(j)}(r), \quad (11)$$

$$Q_s^{(j)}(r) = \sum_{l \neq j}^m \beta^{l \rightarrow j}(r) N_{s-1}^{(l)}(r) + q^{(j)}(r), \quad (12)$$

$$N^{(j)}(r) = \frac{1}{\pi} \int d\psi \int_0^1 \phi^{(j)}(r, \psi, \gamma) d\gamma, \quad (13)$$

the total transport cross-section is

$$a_{tr}^{(j)}(r) = \sum_{l=1}^m \beta^{l \rightarrow l}(r) + a_a^{(j)}(r) \quad (14)$$

the scattering cross-section is

$$\beta^{l \rightarrow j}(r) = \begin{cases} a_0^{l \rightarrow j}(r) & l \neq j \\ a_0^{l \rightarrow l}(r) - a_l^{(l \rightarrow l)} & l = j \end{cases}$$

The functions $a_{tr}^{(j)}(r)$ and $\beta^{1-j}(r)$ are step functions, which are some constants for each velocity group; $q^{(j)}(r)$ is the linear function in the intervals, limited by the knot points of the variable r .

The iterating of the inelastic transitions of S -number consists in the successive solution of equations /10/ for all j with the functions $Q_s^{(j)}(r)$, being known from the previous iteration step of inelastic transitions.

The iteration of the elastic collisions of t -number consists in the solution of the system /10/ for given j with the function $N_{s,t-1}^{(j)}(r)$, obtained in the previous iteration of the elastic scattering. The function $N_s^{(j)}(r)$ as a result of all iterations of elastic collisions is found.

And, at last, by iterating the boundary conditions the function $\phi_{s,r}^{(j)}$ which satisfies the reflection boundary conditions: $\phi^{(j)}(R_{group}, \psi, \gamma) = \phi^{(j)}(R_{group}, \pi - \psi, \gamma)$ is obtained. There is a condition at the outer boundary of a cell in the iterating of the boundary conditions:

$$\phi_{s,t,r}^{(j)}(R_{group}, \psi, \gamma) = \frac{1}{2} [\phi_{s,t,r-1}^{(j)}(R_{group}, \psi, \gamma) + \phi_{s,t,r-1}^{(j)}(R_{group}, \pi - \psi, \gamma)] \quad (16)$$

in all $\pi/2 < \psi < \pi$ interval.

The computational formulas of the S_n -method, needed for solution of the iterated equations (10), were obtained by the general for all geometries scheme, reported in [14]. The approximate solutions of the multigroup system obtained by these formulas satisfy the neutron balance condition. In accordance with this scheme the range of variation of variables r, ψ, γ is covered by a net of knot points (r_k, ψ_i, γ_p) . The knot points γ_p in the interval $[0, 1]$ are chosen as coinciding to Gauss integral formula; the knot points ψ_i in the interval $[0, \pi]$ are chosen as equidistant with the π/n step (the number n coincides the S_n -approximation); the knot points r_k in the interval $[0, R_{group}]$ are chosen arbitrarily, but the condition should be observed, that the points of discontinuity of the functions $a_{tr}^{(j)}(r)$, $\beta^{1-j}(r)$ and $q^{(j)}(r)$ were among r_k - points.

The integral operators $\int_{\pi}^{2\pi} \frac{d\psi}{\psi_i - 1}$ and $\int_{r_{k-1}}^{r_k} r dr$ are successively applied to the equations of system (10) at $\gamma = \gamma_p$ with the assumption of linearity $\phi^{(j)}$ in ψ and r in the intervals $[\psi_{i-1}, \psi_i]$ and $[r_{k-1}, r_k]$. As a result, the algebraical equations we obtain, which connect the values of $\phi^{(j)}$ in knot points.

Adding to this system the equations, obtained after substituting $\psi = \pi$ in (10) with the subsequent application of the operator $\int_{r_{k-1}}^{r_k} r dr$, we have the complete system of equations, from which the values of the functions $\phi^{(j)}(r_k, \psi_i, \gamma_p)$ can be found, using the recurrence formulas.

The realization of the iterating discussed above requires a very large number of iterations. To reduce a number of iterations, we used the corresponding formulas of the acceleration of convergence of iterating.

The convergence of boundary conditions iterating was hastened by extrapolation of the iterative variations of values $\phi_{s,t,r}^{(j)}(R_{group}, \psi_i, \gamma_p)$ / $i=1, 2, \dots, n/2-1$ / on the infinite number of iterations r (Ljusternik method [24]).

The convergence of elastic collision iterations was hastened by the estimation method of iterative deviations [14, 25]. The idea of this method is in the approximate determination of the

iterated function deviation from the exact solution of the equation by its variation after one iteration step. In our case the corresponding formulas can be obtained in the following way. The solution of equation (10) $\phi_s^{(j)}(r, \psi, \gamma)$ can be represented in the form:

$$\phi_s^{(j)}(r, \psi, \gamma) = \phi_{s,t}^{(j)}(r, \psi, \gamma) - \Delta \phi_{s,t}^{(j)}(r, \psi, \gamma) \quad (17)$$

where $\Delta \phi_{s,t}^{(j)}(r, \psi, \gamma)$ is the iterative deviation, corresponding to the iteration of t -number.

Integrating (17) over ψ and γ , we get

$$N_s^{(j)}(r) = N_{s,t}^{(j)}(r) - \Delta N_{s,t}^{(j)}(r) \quad (18)$$

where

$$\Delta N_{s,t}^{(j)}(r) = \frac{1}{\pi} \int_0^\pi d\psi \int_0^1 \Delta \phi_{s,t}^{(j)}(r, \psi, \gamma) d\gamma \quad (19)$$

Using (17) and (18), we obtain from (10):

$$\begin{aligned} \sqrt{1-\gamma^2} \cos \psi \frac{\partial \Delta \phi_{s,t}^{(j)}}{\partial r} - \sqrt{1-\gamma^2} \frac{\sin \psi}{r} \frac{\partial \Delta \phi_{s,t}^{(j)}}{\partial \psi} + a_{tr}^{(j)}(r) \Delta \phi_{s,t}^{(j)} = \\ = \beta j \rightarrow j(r) \Delta N_{s,t-1}^{(j)}(r); \end{aligned} \quad (20)$$

from which the equation for the iterative deviation $\Delta \phi_{s,t}^{(j)}$ follows:

$$\begin{aligned} \sqrt{1-\gamma^2} \cos \psi \frac{\partial \Delta \phi_{s,t}^{(j)}}{\partial r} - \sqrt{1-\gamma^2} \frac{\sin \psi}{r} \frac{\partial \Delta \phi_{s,t}^{(j)}}{\partial \psi} + a_{tr}^{(j)}(r) \Delta \phi_{s,t}^{(j)} = \\ = \beta j \rightarrow j(r) \Delta N_{s,t}^{(j)} + \Delta q_{s,t}^{(j)}(r) \end{aligned} \quad (21)$$

where

$$\Delta q_{s,t}^{(j)}(r) = \beta j \rightarrow j(r) [N_{s,t-1}^{(j)}(r) - N_{s,t}^{(j)}(r)] \quad (22)$$

The boundary conditions of this equation are the previous reflection ones.

The next step is the estimation of the iterative deviation value $\Delta N_{s,t}^{(j)}(r)$ or, in other words, the approximate solution of equation (21). From the fact, that with $\phi_{s,t}^{(j)} \rightarrow \phi_s^{(j)}(r)$ the function $\Delta \phi_{s,t}^{(j)} \rightarrow 0$ and becomes more smooth, we obtain the equation for an estimation of iterative deviation $\tilde{\Delta \phi}_{s,t}^{(j)}(r, \psi, \gamma)$:

$$\sqrt{1-\gamma^2} \cos \psi \frac{\partial \tilde{\Delta \phi}_{s,t}^{(j)}}{\partial r} - \sqrt{1-\gamma^2} \frac{\sin \psi}{r} \frac{\partial \tilde{\Delta \phi}_{s,t}^{(j)}}{\partial \psi} + a_{tr}^{(j)}(r) \tilde{\Delta \phi}_{s,t}^{(j)} = \Delta q_{s,t}^{(j)}(r); \quad (23)$$

No iterations of the elastic collisions are needed for the solution of this equation.

The approximate function of average flux, thus obtained:

$$N_{s,t}^{(j)}(r) = N_{s,t}^{(j)}(r) - \Delta N_{s,t}^{(j)}(r) \quad (24)$$

where

$$\Delta N_{s,t}^{(j)}(r) = \frac{1}{\pi} \int_0^\pi d\psi \int_0^1 \tilde{\Delta \phi}_{s,t}^{(j)}(r, \psi, \gamma) d\gamma \quad (25)$$

is used then as a new approximation in iterated equation (10). All iterating and introducing of iterative corrections last till the ratio $\Delta N_{s,t}^{(j)}(r)$ for all r becomes less than the value ϵ .

As the function $\Delta\tilde{\phi}_{s,t}(r)$ gives only approximate value of the iterative deviation $\phi_{s,t}^{(i)}$ from the exact solution $\phi_s^{(0)}$, then to reduce numerical work, it must be determined in more low-order approximations in comparison to the approximations, used in calculation of $\phi_{s,t}^{(i)}$ itself.

In cases when the conditions for introducing of the correction from (24) were not held, the convergence of elastic collision iterating was hastened by the factorization of the iterated function by the balance normalization factor. The same acceleration of convergence was applied to inelastic transition iterating.

III. MONTE CARLO CALCULATION OF NEUTRON FLUX.

Using the probability characteristics of neutron interactions with nuclei and those of the cell geometry, the neutron wandering in the cell is modeled by means of a digital computer machine. At the cell boundary a neutron is reflected mirrorly with no velocity change. The source in the thermalization range is constructed with the assumption, that for velocities $v > v_{\text{group}}$ a neutron is scattered (elastically and isotropically in the centre mass system) by fixed free nuclei and that at $v < v_{\text{group}}$ the neutron spectrum is Fermi spectrum.

All probability characteristics of neutron interactions can be tabulated, but it needs a large volume of an operative computer memory.

In the case of a gas model for moderator the neutron scattering by nuclei of a certain type can be modeled as follows. The absolute value of the velocity V_0 of nuclei with which neutron collides, is selected. For this purpose in relation to V_0 the following equation is solved

$$K = \begin{cases} \frac{1}{\beta^2} \phi_4(\gamma) + 3\phi_2(\gamma), & \gamma \leq \beta \\ \frac{1}{\beta^2} \phi_4(\gamma) + 3\phi_2(\beta) + \frac{3}{\beta} [\phi_3(\gamma) - \phi_3(\beta)] + \beta [\phi_1(\gamma) - \phi_1(\beta)] & \gamma > \beta \end{cases}$$

$$\frac{1}{\beta^2} \phi_4(\gamma) + 3\phi_2(\beta) + \frac{3}{\beta} [\frac{1}{2} - \phi_3(\beta)] + \beta [\frac{1}{2} - \phi_1(\beta)]$$

where $\beta = V/V_T$, $\gamma = V_0/V_T$, V is the neutron velocity, V_T is the most probable nuclear velocity at the temperature $T^\circ K$, K is a random number, $0 < K < 1$, $\phi_n(z) = \int_0^z t^n e^{-t^2} dt$. The functions $\phi_n(z)$ are to be computed beforehand.

Then the angle θ between the neutron motion and the nucleus as a target direction is selected:

$$\cos \theta = \frac{1}{2a} \{ 1 + a^2 - [K(1+a)^3 + (1-K)|1-a|^3]^{2/3} \},$$

$a = V_0/V$. The second angular parameter is determined from the condition of equivalence of azimuthal directions. From the known neutron and nuclear velocities \vec{V} , \vec{V}_0 the velocity of a scattered neutron is calculated by

$$\vec{V}' = \frac{1}{M+1} [\vec{V} + M\vec{V}_0 + M|\vec{V} - \vec{V}_0|\vec{e}]$$

\vec{e} is a random isotropic unit vector.

It is known a number of ways to store the information on the flux during the neutron wandering [25]. As a rule, the spectrum in the moderator is rapidly established. The difficulties are connected with greatly absorbing domains of a small volume. The calculation of the flux in any part of the cell may be significantly hastened, if one takes into account the contribution of each collision; after which a possible path of neutron scattered crosses its volume. In the cells with moderator volume predominance the computations can be significantly accelerated when replacing the moderator regions, remote from the block, by the corresponding surface sources. The characteristics of sources (spectrum, angular distribution etc) are to be computed beforehand. In onedimensional cells it is realized in an especially simple way. The graphite-uranium cell was computed by this method (page 13).

As a rule, to get the exactness of computation, practically accepted, $(7-10) \cdot 10^4$ collisions are sufficient. The results of computations, in which more than 10^5 collisions were selected, are shown in Figs 12, 13. As for spectrum in graphite (Fig. 13b) further corrections were made. Below the approximate values of standard errors of some characteristics of the fluxes computed are represented (in %):

Cell	Zone	(1)	(2)	(3)	(4)	(5)	(6)	(7)
Uranium-water	Block	0.89	0.83	2.2	1.4	2.4	5.9	3.6
	Moderator	0.14	0.36	0.94	0.55	1.1	2.3	2.1
Uranium-graphite	Block	0.73	0.89	2.9	1.3	1.9	2.4	3.5

(1) — total flux, (2) — total absorption, (3), (4), (5), (6), (7), — fluxes of variable $x = V/\sqrt{2kT_0}$ in intervals (0.1), (1.2), (2.3), (3.4), (4.8), respectively, $T_0 = 300^\circ\text{K}$.

In computations three-order generator of pseudorandom numbers of a known type: $X_{p+1} = pX_n \pmod{M}$ was used. We put $p=55$, $M=2^{24}$, $X_0=1$ and $X_0=3$. The generator was tested by the computation of Maxwellian spectrum in a cell, with no absorption taken into account, and by Kolmogorov criterion ρ , ω^2 at the different sample sizes.

The results are satisfactory.

It is useful to smooth the density functions, obtained by statistical method. The following way is very useful too [26]. The empirical function of probability distribution $F(x)$, corresponding to the calculated density function, is considered. At the knot point X_k , $k=s, s+1, \dots, n-s$ ($n+1$ is the total number of knots) $F(x_k)$ is replaced by $P(x_k)$, where $P_s(x)$ is a polynomial of certain degree, which minimizes the value $\sum_{i=-s}^s [F(x_{k+i}) - P(x_{k+i})]^2$. By differentiating a more smooth distribution function, thus constructed, the smoothed density function is obtained. We used the polynomials of the fifth degree at $s=8/n=80/$.

IV. RESULTS OF CALCULATIONS

The described above methods were used for the calculation of the space-energy slow neutron distribution along the cells of uranium-water and uranium-graphite lattices, studied experimentally by Mostovoi [6,7].

The uranium-water assembly is a set of blocks of natural uranium 3.5cm in diameter, located in the sites of a triangular lattice with the 5.5cm spacing.

The uranium-graphite assembly consists of the same uranium blocks, located in the sites of a square lattice with 20cm spacing. In the experiments the uranium blocks are separated by an aluminium layer from the moderator.

In calculations the experimental hexagonal and square cells were replaced by the equivalent circular threezone cells.

Now we proceed to describing the calculations of cells in P_3 - approximation. The calculation of slow neutron flux was performed in the energy range $0 < E < E_{\text{group}} = 0.67$ eV in 15-group approximation. The sources of thermal neutrons caused by slowing down were calculated with the assumption, that at $E > E_{\text{group}}$ the neutron spectrum is Fermi spectrum and molecular binding effect at $E > E_{\text{group}}$ is not of importance. The inelastic molecular scattering and neutron interaction with the crystal lattice at $0 < E < E_{\text{group}}$ were taken into account on the basis of Turchin results [22,23].

For fissionable isotopes the deviation of the capture cross-section from $1/v$ law was taken into account.

The space distributions of average thermal neutron flux are given in Figs 2,3.

$$\Phi_{00}(r) = \frac{1}{4\pi} \int_0^{v_{\text{group}}} dv \int \phi(r, v, \theta, \psi) d\Omega,$$

and also directed fluxes /see (8)/:

$$\begin{aligned} \Phi_{11}(r) &= \int_0^{v_{\text{group}}} \phi(r, v, \theta = 0) dv, \quad \Phi_{\perp}^{(0)}(r) = \int_0^{v_{\text{group}}} \phi(r, v, \theta = \frac{\pi}{2}, \psi = 0) dv, \\ \Phi_{\perp}^{(\pi)}(r) &= \int_0^{v_{\text{group}}} \phi(r, v, \theta = \frac{\pi}{2}, \psi = \frac{\pi}{2}) dv, \quad \Phi_{\perp}^{(\pi)}(r) = \int_0^{v_{\text{group}}} \phi(r, v, \theta = \frac{\pi}{2}, \psi = \pi) dv \end{aligned}$$

It is seen from Figs 2 and 3, that neutron flux $\Phi_{11}(r)$ (neutron velocities are parallel to a cell axis) is "eaten out" much stronger in the block, than the average flux $\Phi_{00}(r)$. From physical point of view, this results from the fact, that the capture probability of neutrons moving in a block along its axis, is greater, than for neutrons of other directions. As the distance from block increases, $\Phi_{11}(r)$ becomes larger, than $\Phi_{00}(r)$, and this fact can be also simply explained from physical point of view.

Let us discuss in detail curve 3 (Figs 2 and 3). It describes a neutron beam, directed along a cell diameter. The left branch of this curve ($r < 0$) corresponds to the neutrons, moving towards the cell axis, $\Phi_{\perp}^{(\pi)}(r)$, and right one does to the neutrons moving in an opposite direction $\Phi_{\perp}^{(0)}(r)$. In the most part of its path in a block, the neutron beam loses, as a result of capture, more neutrons, than acquires from other beams due to scattering. This results in a monotone character of curve 3 in a block. The disturbance of the beam monotony when leaving the block is connected with the general increase of neutron density near the block boundary. Crossing the aluminium layer, the beam $\Phi_{\perp}^{(0)}(r)$ does not considerably change due to absorption and scattering, and the abrupt decrease of curve 3 in a layer is due to its geometry.

The distribution along diameter of those neutrons, velocities of which are perpendicular to an axial cross-section of the cell, $\phi_{\perp}(\pi/2)(r)$ is represented by curve 4 in Fig. 2. It is evident, that at $r=0$ $\phi_{\perp}(0)(0)=\phi_{\perp}(\pi/2)(0)=\phi_{\perp}(\pi)(0)$.

Now we proceed to an analysis of the thermal neutron energy spectra in cells /Figs 4-9/. The abscissa is plotted in variable $1/x$ ($x=v/\sqrt{2kT}$, $T=300^{\circ}\text{K}$). The ordinata is the neutron density $n(1/v)=v^2n(v)=v\phi(v)$. In Figs 4,6,8 the neutron spectra at the centre of the cell are shown. The curve 1 represents the neutron energy distribution, averaged over the angles

$\frac{1}{4\pi} \int v\phi(r=0, v, \theta) d\Omega$. The curve 2 corresponds to neutron beam energy distribution along the cell axis $v\phi(r=0, v, \theta=0)$ and curve 3 presents the spectrum of the neutron beam perpendicular to the cell axis $v\phi(r=0, v, \theta=\pi/2)$. From physical considerations spectrum 2 is to be harder than global spectrum 1, but spectrum 3 - softer.

It is well in agreement with the calculations. The spectra given are compared with experimentally measured ones. The experimental method was such that the beams extracted from the blocks were mainly of neutrons, directed along the axis of the cell. It is natural therefore to compare the experimental spectra with the functions $v\phi(r=0, v, \theta=0)$.

However, one should expect that the experimental spectrum will be a bit softer than the theoretical one, since the neutron beam extracted has the neutrons of other directions. In the uranium-water cell this prediction is confirmed by the calculation. In the uranium-water cell this effect is weak due to a considerable softening of the spectrum calculated in the moderator as compared with the experiment. The origin of this softening is not yet clear.

The comparison of the same experimental spectrum with the global spectrum $\frac{1}{4\pi} \int v\phi(r=0, v, \theta, \psi) d\Omega$ reveals that the experimental one is harder. In Figs 5,7,9 the comparison of the theoretical and experimental spectra at the cell boundary is given. Calculations show the neutron flux at the cell boundary is practically isotropic. Figs 10,11 present space and energy distribution of the neutron importance in relation to the absorption in a block for the uranium-water cell. The presence of maxima in the curves 1 and 2 (Fig. 11) in the range $3.0 < x < 4.0$ is caused by the resonance in the absorption cross-section σ_{235} . It is of interest to confront all the three methods given above. For this purpose the thermal neutron fluxes in uranium-water and uranium-graphite cells were calculated by each method. The computations were made on the basis of gas model, since in this case the scattering indicatrix can be selected by Monte Carlo method completely. The results of the computations are shown in Figs 12 and 13. The mutual attachment of the spectra calculated by different methods was made in the block, as well as in the moderator at the maximum. There is a good agreement between the spectra given within the errors of the methods.

We are much obliged to Dr. V.J. Mostovoi and Dr. V.S. Dikarev for their interest in the present work and useful discussions during its realization.

LIST OF REFERENCE

1. H. Ilurwitz, M.S. Nelkin, G.I. Habetler, *J. Nucl. Sci. and Eng.*, 1, 280 (1956).
2. E. Cohen, *Collection, Experimental Reactors and Reactor Physics (Translation of the First Geneva Conference Paper No 611 / GITTL, 1956.*
3. E. Cohen, *J. Nucl. Sci. and Eng.*, 2, 227 (1957).
4. M.V. Kazarnovski et al. *Transactions of the Second International Conf. on the Peaceful Uses of Atomic Energy, Reports of Soviet scientists, Atomizdat*, 2, 651 (1959).
5. *Proceedings of the Brookhaven Conference on Neutron Thermalization*, 1-4 (1962).
6. V.I. Mostovoi et al, *Atomnaya energiya, /Atomic energy/* 13, 547 (1962).
7. V.I. Mostovoi, V.S. Dikarev et al. *The report presented at the Third Intern. Conf. on the Peaceful Uses of Atomic Energy*, 1964.
8. G.A. Bat, E.A. Grigorieva et al. *The report presented at the Third Int. Conf. on the Peaceful Uses of Atomic En.*, 1964.
9. V. Vladimirov, *Collection, Vychislitel'naya matematika /Computational mathematics/ No 3,3, (1958).*
10. G.I. Marchuk et al, *Atomnaya energiya* 13, 534 (1962).
11. L.I. Maiorov, M.S. Judkevitch, *Atomnaya energiya*, 13, 563 (1962).
12. B.G. Carlson, *Los Alamos Scientific Laboratory report LA 1891 (1955).*
13. B.G. Carlson and J. Bell, *Collection, Transactions of the Second Inter. Conf. on the Peaceful Uses of Atomic Energy, Reports of foreign scientists, Moscow, Atomizdat*, 3, 406, (1959).
14. V.N. Morozov, *Collection, Teoria i metody rascheta yadernykh reaktorov /Theory and Methods of Calculation of Nuclear Reactors/, Gosatomizdat*, (1957).
15. A.D. Galanin, *Teoria yadernykh reaktorov na teplovykh neitronah /Theory of Thermal Neutron Nuclear Reactors/ Atomizdat*, (1957).
16. G.I. Marchuk et al., *Proceedings of the Brookhaven Conference on Neutron Thermalization*, 2, (1962).
17. Takahashi H.J., *Nucl. Sci. and Eng*, 5, 338, (1959).
18. G.I. Marchuk, *Metody rascheta yadernykh reaktorov /Methods of Calculating Nuclear Reactors/, Atomizdat*, (1961).
19. L.N. Usachev, *Collection, Yadernie reaktory i fizika reaktorov /Nuclear Reactors and Reactor Physics/, AN SSSR*, 251, 1955.
20. G.I. Marchuk and V.V. Orlov, *Collection, Neitronnaya fizika, Gosatomizdat*, 1961.
21. S. Glasstone and M.G. Edlund, *The elements of nuclear reactor theory*, Toronto-New York-London, 1952.
22. V.F. Turchin, *Proc. of Symposium, Vienna*, 259, 1960.
23. V.F. Turchin, *Medlennye neitrony (Slow Neutrons/ Gosatomizdat*, 1963.
24. L.A. Lyusternik, *Trudy matematicheskogo instituta AN SSSR /Transactions of the Institute of Academy of Sciences, USSR/ Izd. AN SSSR*, 49, (1947).
25. N.P. Busienko et al. *Metod statisticheskikh ispytani /Method of statistical tests/, Fizmatgiz*, 1962.
26. K. Lanzosch, *Practicheskie metody prikladnogo analiza /Practical methods of applied analysis/, Fizmatgiz*, 1961.

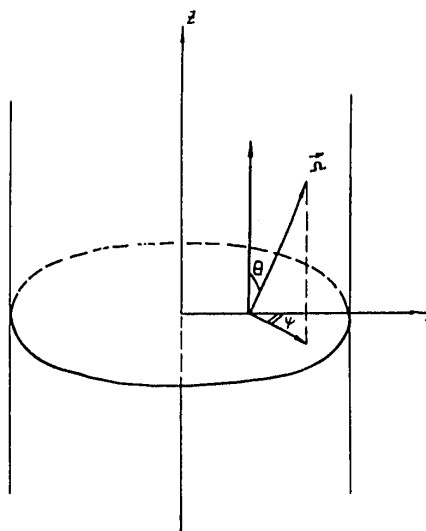


Fig.1.

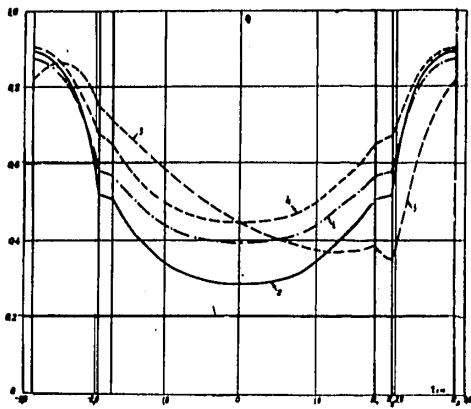


Fig. 2.

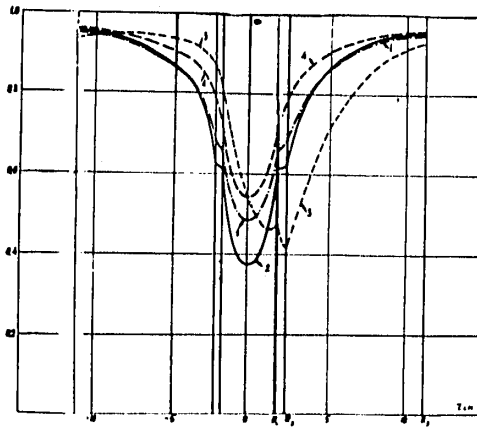


Fig. 3.

Space distribution of thermal neutrons in cells (Fig. 2-uranium-water cell, $T=323^{\circ}\text{K}$; Fig. 3-uranium-graphite cell, $T=523^{\circ}\text{K}$).

$$1 - \phi_{\text{w}}(z); \quad 2 - \phi_{\text{g}}(z); \quad 3 - \begin{cases} \phi_{\text{w}}^{(1)}(z) & (z=0) \\ \phi_{\text{w}}^{(2)}(z) & (z=1) \end{cases}; \quad 4 - \phi_1^{(2)}(z)$$

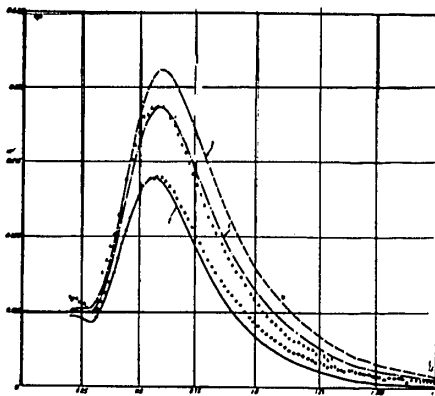


Fig. 4. Energy distribution of thermal neutrons at the centre of uranium-water cell ($T=323^{\circ}\text{K}$).

$$1 - \frac{1}{4\pi} \int v\varphi(z=0, v, \theta) d\Omega; \quad 2 - v\varphi(z=0, v, \theta=0); \\ 3 - v\varphi(z=0, v, \theta=\pi/2).$$

o-experimental spectrum, normalized to the maximum of the curve 2.
 Δ -the same spectrum, normalized to the maximum of curve 1.

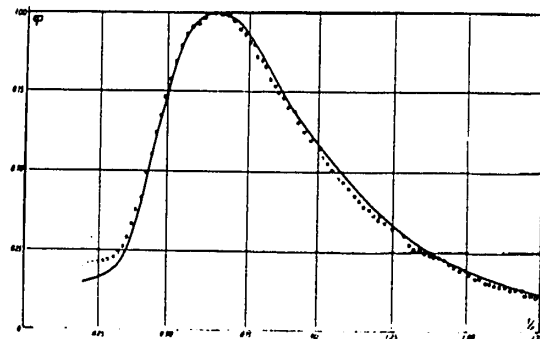


Fig. 5. Energy spectrum of thermal neutrons at the boundary of uranium-water cell ($T=323^{\circ}\text{K}$).

— calculated curve
 o-experimental points

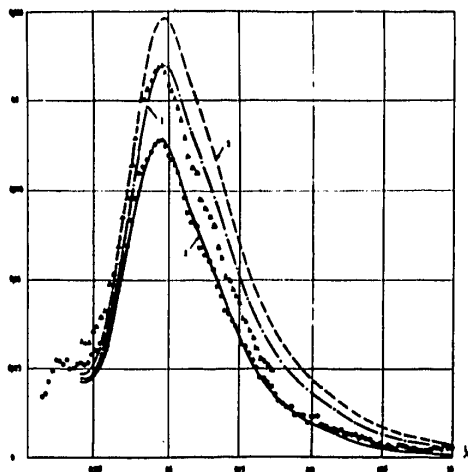


Fig. 6.

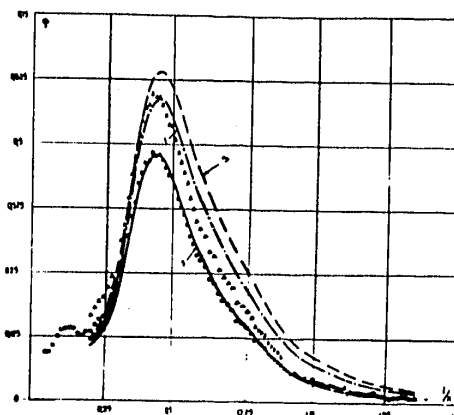


Fig. 8.

Energy distribution of thermal neutrons at the centre of uranium-graphite cell (Fig. 6- $T=523^\circ\text{K}$; Fig. 8- $T=613^\circ\text{K}$)

$$1 - \frac{1}{4\pi} \int \psi(r=0, \vartheta, \varphi) d\Omega; \quad 2 - \psi(r=0, \vartheta, \varphi=0);$$

$$3 - \psi(r=0, \vartheta, \varphi = \pi/2)$$

o- experimental spectrum, normalized to the maximum of the curve 2;
 Δ- the same spectrum, normalized to the maximum of the curve 1.

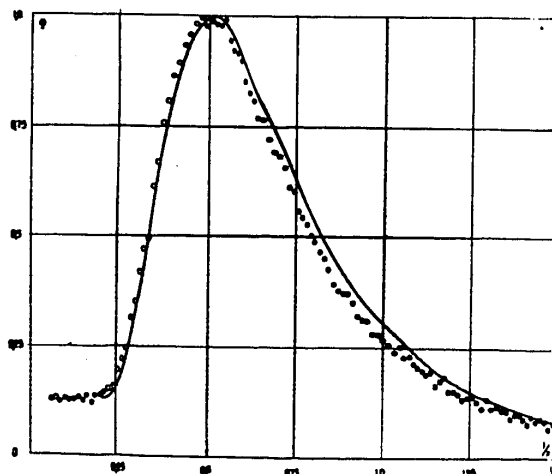


Fig. 7.

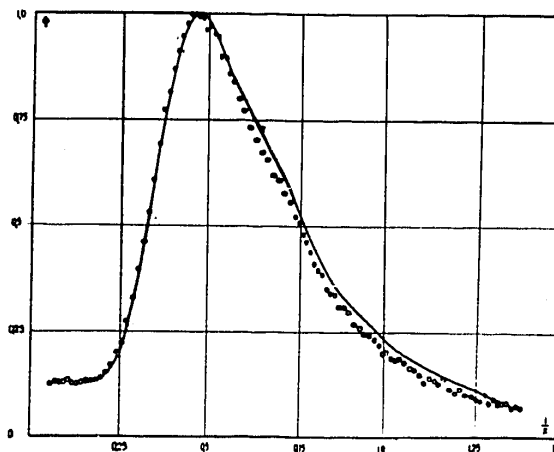


Fig. 9.

Energy distribution of thermal neutrons at the boundary of uranium-graphite cell (Fig. 7- $T=523^\circ\text{K}$; Fig. 9- $T=613^\circ\text{K}$).

— calculated curve
 o- experimental points

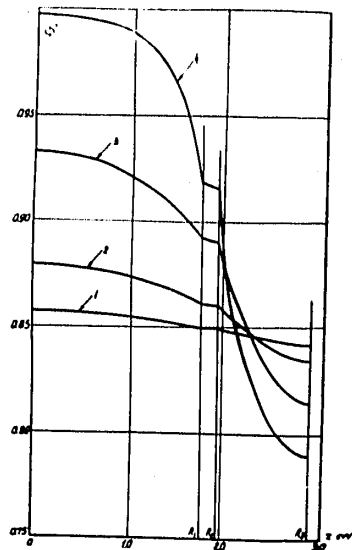


Fig. 10. Space distribution of neutron importance function (in relation to the capture in the block) in the uranium-water cell.

1 - $\phi^*(z, E = 0.6 \text{ eV})$; 2 - $\phi^*(z, E = 0.17 \text{ eV})$;
3 - $\phi^*(z, E = 0.028 \text{ eV})$; 4 - $\phi^*(z, E = 0.0006 \text{ eV})$.

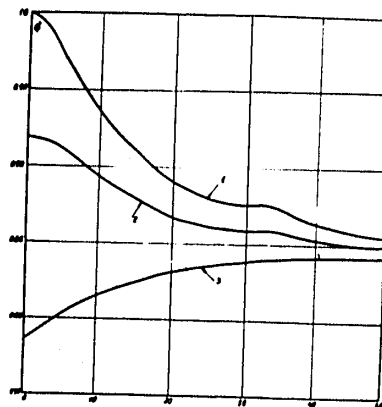


Fig. 11. Energy dependence of neutron importance (in relation to the capture in the block) in the uranium-water cell.
1 - at the centre of the block,
2 - at the block boundary,
3 - at the boundary of the cell.

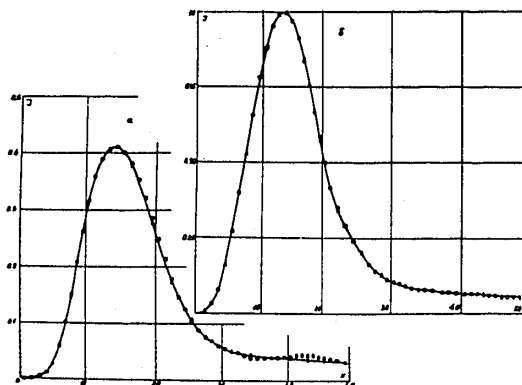


Fig. 12.

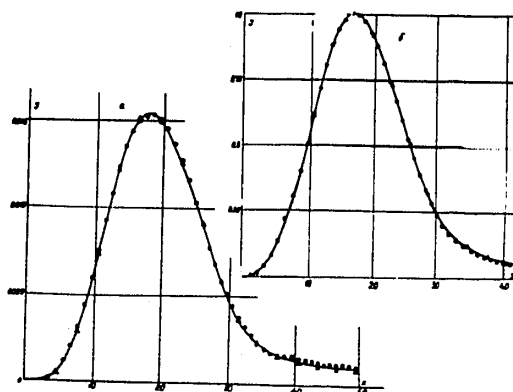


Fig. 13.

Comparison of the neutron energy spectra, calculated by different methods (Fig. 12-uranium-water cell, $T=323^\circ\text{K}$; Fig. 13-uranium-graphite cell, $T=523^\circ\text{K}$).

— calculation by the spherical harmonics method (P_3 -approximation, 15 groups), Δ -calculation by S_8 method (S_8 -approximation, 10 groups). \circ - Monte-Carlo calculation.
a) neutron spectrum in the block volume
b) neutron spectrum in the moderator volume